Silicon (2024) 16:3033–3039
https://doi.org/10.1007/s12633-024-02914-z

RESEARCH

Theoretical Examination of the Radiation Shielding Qualities of MgO-PbO-SiO_2-B_2O_3-BaO Glass Systems

M. I. Sayyed[1,2]

Received: 6 January 2024 / Accepted: 9 February 2024 / Published online: 15 February 2024

Abstract

Melt quenching method was used to prepare a glass series composed of 5MgO-20PbO-10SiO_2-(65-x)B_2O_3-xBaO, (x = 10, 15, 20 and 25 mol%), with the resulting glasses' capacity for radiation shielding explored through Phy-X software. The mass attenuation coefficients (MAC) were examined in the 0.122–1.485 MeV energy range, with 0.122 MeV the resulting maximum value and a 1.557–1.611 cm^2/g variation. At the low energy range, a clear relationship between the MAC and the energy emerged, with 0.054 cm^2/g at 0.122 MeV representing the MAC difference between the lowest and highest BaO-content glasses. Conversely, at the high energy range, the influence of BaO on the MAC diminished considerably, whereby the MAC difference between the two glasses was a mere 0.001. We evaluated the prepared glasses' linear attenuation coefficients (LAC), finding a direct relation between the LAC and glass density. At 0.245 MeV, the LAC values were 1.425, 1.486, 1.546, and 1.607 cm^{-1} at the respective densities of 4.275, 4.438, 4.601, and 4.764 cm^{-1}. According to the LAC results, the glass with the composition of 5MgO-20PbO-40 B_2O_3-10SiO_2-25BaO has the more desirable shielding properties. We observed a decrease in the TF with increasing the amount of BaO in the prepared glasses. This observation implies that BaO has an important role in enhancing the glasses' radiation shielding ability.

Keywords Borosilicate glasses · Lead oxide · Radiation shielding glasses · Attenuation factors

1 Introduction

Significant focus has been placed on glass composites in the domain of materials science as a result of their potential application in diverse contexts such as aerospace, medical devices, and optics [1–4]. Borosilicate glass composites represent advanced materials whereby borosilicate glass, characterized by exceptional durability and thermal resistance, is combined with other oxides to create materials with unique properties that include chemical resistance, high transparency, mechanical strength, and radiation shielding [5, 6].

Melt quenching is a technique employed in glass fabrication that entails the heating of a raw materials' mixture until melting occurs and a homogeneous liquid is formed. Then, the liquid is cooled rapidly to solidify it and create an amorphous glass structure. This technique enables glass to be produced with specific compositions and properties, rendering this an important process in terms of developing materials for advanced applications [7, 8].

Due to the increasing concerns regarding the harmful impacts of exposure to ionizing radiation in the myriad settings where it is either present or generated, it is essential that materials can be developed that have the capacity to offer shielding protection [9–13]. The present investigation places its lens of focus on exploring the efficacy of the MgO-PbO-B_2O_3-SiO_2-BaO glass system in order to determine its ability to shield against ionizing radiation.

Insight into glass materials' structural nuances is vital to enable their behavior and properties under varying conditions to be precisely controlled, thus ensuring the reliability and safety of the applications in which the materials are deployed [14]. This study explores the arrangement of the MgO-PbO-B_2O_3-SiO_2-BaO glasses at the atomic and molecular levels in order to shine a light on the relationships between the structure of the glasses and their ability to shield against radiation.

✉ M. I. Sayyed
dr.mabualssayed@gmail.com

[1] Department of Physics, Faculty of Science, Isra University, Amman, Jordan

[2] Renewable Energy and Environmental Technology Center, University of Tabuk, 47913 Tabuk, Saudi Arabia

Metal oxides have significance in terms of influencing the glass's characteristics by acting as formers or network modifiers to impact the properties and structure (e.g. hardness, thermal expansion, and transparency). Modifiers such as magnesium oxide (MgO) can enhance the workability and reduce the melting point, while formers like silicon dioxide (SiO_2) contribute towards the glass's stability and chemical/heat resistance. Therefore, the glass's characteristics can be carefully controlled by tailoring the metal oxides' composition [15, 16].

As a glass former, boric oxide (B_2O_3) with heavy metal oxides has a noteworthy capacity to shield against gamma radiation [17, 18]. Therefore, B_2O_3 is incorporated into the MgO-PbO-SiO_2-BaO glass system in the present investigation in order to determine this former's influence on the attenuation of gamma rays.

The computational approach, via software such as Phy-X, allows radiation-shielding characteristics to be quantitatively analyzed through the simulation of radiation's interaction with the target materials. For example, using data and mathematical models, Phy-X can calculate the absorption, attenuation, and radiation scattering that manifests within various shields [19, 20]. This study thus seeks to gain greater insight into the radiation-shielding characteristics of MgO-PbO-B_2O_3-SiO_2-BaO glasses through the prediction and validation of the attenuation coefficients using advanced computational methods.

Comparative analysis will serve as a benchmark for the evaluation of the MgO-PbO-B_2O_3-SiO_2-BaO glasses' efficacy by conducting a systematic comparison of their properties with those of other glass compositions. Such analysis will shine a light on the glasses' specific advantages and limitations, thus supporting informed decision-making in terms of the selection of those materials most suited for specific applications in radiation-rich settings, and optimizing the materials' cost-effectiveness and performance [21, 22]. Besides conducting a theoretical study, this investigation will also underscore the MgO-PbO-B_2O_3-SiO_2-BaO glass system's practical implications. Determination of the glasses suitability for use in medical and nuclear contexts, as well as in space exploration, will lead to important understanding, creating a practical link between the theoretical findings and actual deployment and use in the field [23]. This significance of this study involves its contribution to advanced materials for radiation-shielding purposes. Through examining the association between the target glass system's composite materials, radiation-shielding ability, and structure, the ground is laid for future investigation. Future research opportunities will help to address concerns regarding radiation exposure and leakage by carrying out practical experiments, as well the potential to introduce new compounds, and employing computational techniques to optimize the composition of the target glasses. In this study, new glasses are prepared with the chemical formula 5MgO-20PbO-10SiO_2-(65-x) B_2O_3-xBaO, x = 10, 15, 20 and 25 mol%, and their ability to shield against radiation investigated.

2 Materials and Methods

2.1 Glass Samples Preparation

In this work, we prepared 5MgO-20PbO-10SiO_2-(65-x)B_2O_3-xBaO, (x = 10, 15, 20 and 25 mol%) glasses via the widely employed technique of melt quenching. Briefly, a total of four glass samples were fabricated using the chemical powders B_2O_3, MgO, PbO, SiO_2 and BaO. After weighing the necessary chemicals, a 20 g batch of each glass powder was mixed thoroughly. It was then melted for 2 h at 1100 °C in a high-temperature electrical furnace using a high-purity alumina crucible. To eliminate internal stresses, annealing of the glass samples was carried out for 3.5 h at 400 °C in another furnace. For convenience, the samples were labeled as "S1" (x = 10 mol%), "S2" (x = 15 mol%), "S3" (x = 20 mol%), and "S4" (x = 25 mol%), with Table 1 summarizing the glasses' chemical composition.

2.2 Radiation Shielding Features

To calculate the prepared samples' radiation shielding properties, the Phy-X software [24] was employed. The evaluation of these shielding factors facilitates studying the selected glasses' ability to attenuate radiation. Expressing the attenuation of the photon beam intensity when travelling through a glass sample can be achieved via the Lambert–Beer law. Mathematically, we can write this basic equation as:

$$I = I_0 e^{-\mu . x} \tag{1}$$

where, I_0 and I are respectively the photon's unabated and attenuated intensities, x is the thickness (in cm) and μ (or LAC) is the linear attenuation coefficient (in cm^{-1}).

We can rewrite Eq. 1 as:

$$MAC = \frac{1}{\rho x} ln\left(\frac{I_0}{I}\right) \tag{2}$$

Where MAC denotes the mass attenuation coefficient.

Table 1 The chemical composition of the glasses

Sample	MgO	PbO	B_2O_3	SiO_2	BaO
S1	5	20	55	10	10
S2	5	20	50	10	15
S3	5	20	45	10	20
S4	5	20	40	10	25

With the glasses composed of differing elements, the MAC can be estimated for any sample using the mixture rule, which can be represented as:

$$(MAC)_{glass} = \sum_i W_i (MAC)_i \quad (3)$$

The MAC is a crucial quantity for a given media since it allows us to estimate the LAC. Using Eq. 4, we can easily relate the MAC and LAC for a medium:

$$LAC = MAC \times density \quad (4)$$

The half value layer (HVL) is the absorber thickness that leads to a 50% reduction in the intensity of the incoming radiation, namely:

$$HVL = \frac{ln2}{LAC} \quad (5)$$

The literature provides further information about various materials' radiation shielding characteristics [25–42].

3 Results and Discussion

As an initial determination of the glasses' shielding abilities, the materials' MAC values are graphed against various energies in Fig. 1. The highest MAC values are noted at 0.122 MeV, the lowest energy tested, dropping down until the minimum values of the tested range are reached at 1.458 MeV. More specifically, the S2 sample's MAC is 1.576 cm^2/g at 0.122 MeV, decreasing to 0.147 cm^2/g at 0.411 MeV, 0.072 cm^2/g at 0.867 MeV, and 0.051 cm^2/g at 1.458 MeV. The MAC values also reveal how close this parameter determines the glasses' shielding abilities. This difference is at its greatest at low energies, namely 0.054 cm^2/g at 0.122 MeV, while the difference between the lowest and highest MAC value is within 0.001 cm^2/g at higher energies. Thus, the materials have relatively similar attenuation abilities at most energies.

To further evaluate the samples, in Fig. 2 the LAC of the glasses were calculated at several energies as a function of the glass system's densities, revealing that at almost every energy tested, the greater the sample density, the higher the LAC value. For example, at 0.245 MeV, the LAC values are 1.425, 1.486, 1.546, and 1.607 cm^{-1} at densities of 4.275, 4.438, 4.601, and 4.764 cm^{-1}, respectively, while at 1.112 MeV the LAC values are 0.260, 0.268, 0.276, and 0.285 cm^{-1} at the same respective densities. By introducing more BaO into the samples while reducing the B_2O_3 content, the density of the overall system increases, leading to greater attenuation and a better shield. Because of this, these findings show the S4 glass to have the superior shielding qualities. It should also be noted that even though at all energies the S4 sample has the highest LAC value, we must explain other parameters to confirm that this glass sample is more preferable in radiation shielding applications.

Figures 3 and 4 illustrate the glasses' TF values against energy with 0.5 and 1 cm thickness, respectively. Focusing on Fig. 3 first, the glasses have an increasing trend with energy. At 0.122 MeV, the lowest TF values are found in the 0.026–0.036 range. Meanwhile, at the highest tested energy, 1.458 MeV, the TF values are in the 0.886–0.896 range. This rapid increase is caused by higher energy photons being able to penetrate through more of the samples at a set thickness. To decrease the amount of transmission, the BaO content in the glasses can be raised. For example, at 0.444 MeV, the TF values are equal to 0.751, 0.744,

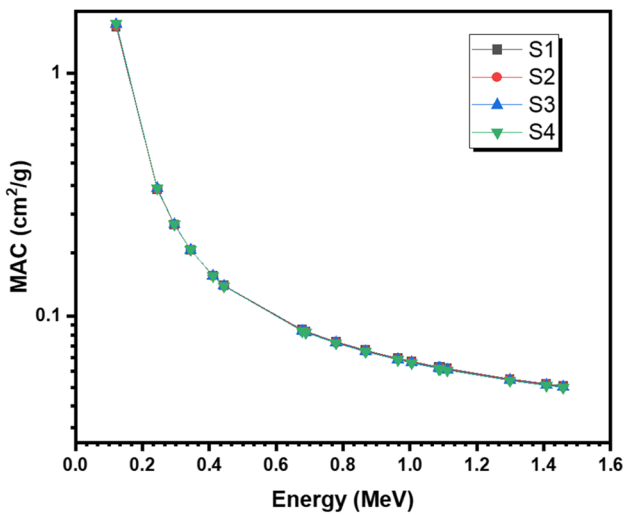

Fig. 1 The mass attenuation coefficient for the prepared glasses

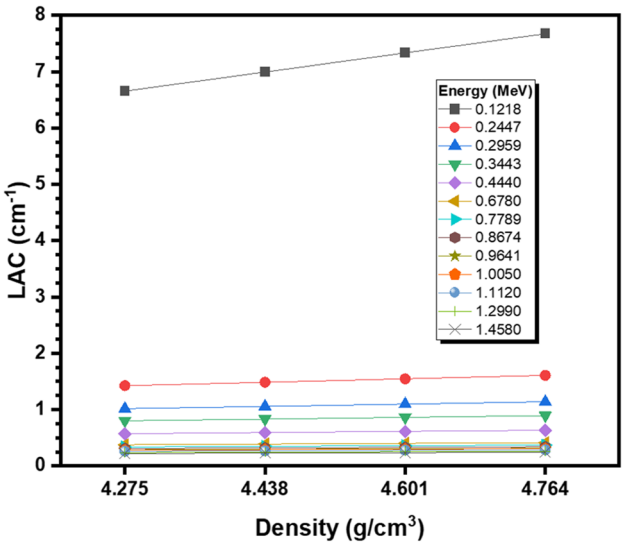

Fig. 2 The linear attenuation coefficient as a function of the density

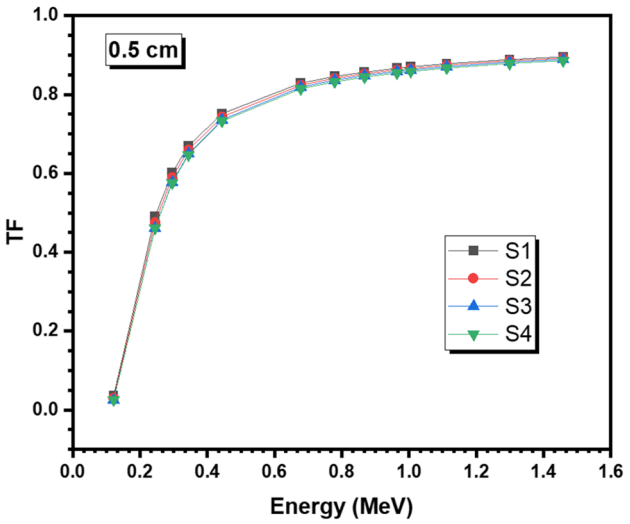

Fig. 3 The transmission factor values of the glasses against energy with a thickness of 0.5 cm

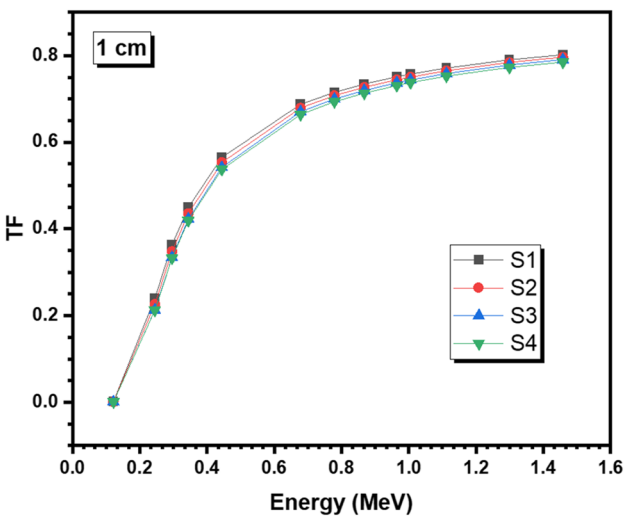

Fig. 4 The TF values of the glasses against energy with a thickness of 1 cm

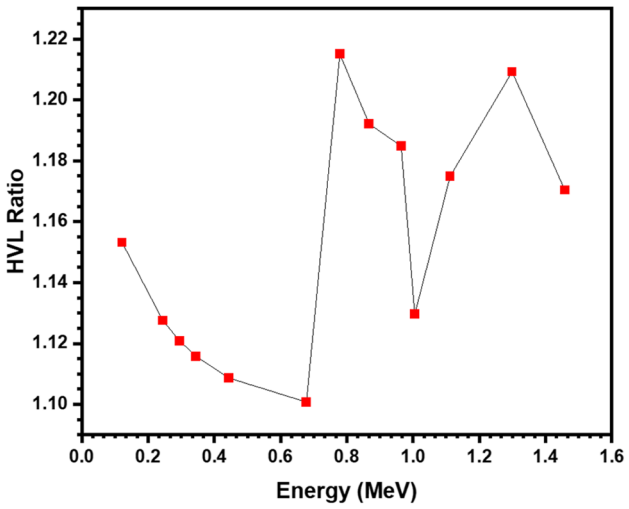

Fig. 5 The ratio of half value layer values between the S1 glass and S4 glass at several energies

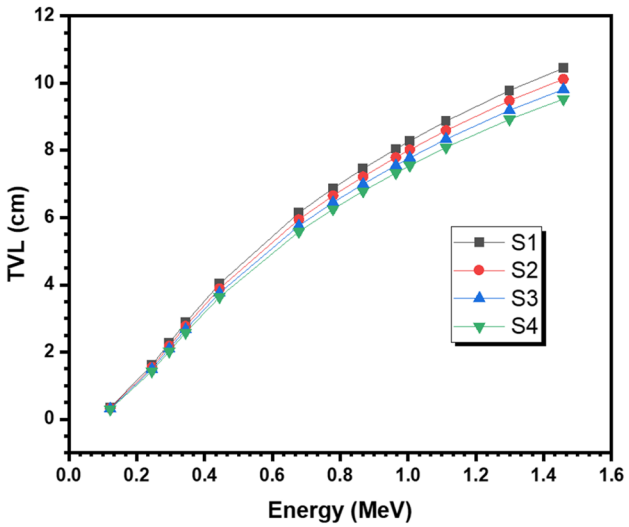

Fig. 6 The tenth value layer of the samples against energy

0.736, and 0.733 for S1-S4, respectively, while at 1.112 MeV they are 0.878, 0.875, 0.871, and 0.867, respectively. Thus, the S4 sample, having the highest BaO content, has the best shielding ability. If further attenuation is needed, the thickness of the samples needs to be raised. Figure 4 illustrates this increase from 0.5 to 1 cm, where all the TF values decrease for their respective energies and samples. For instance, at 1.458 MeV, the highest TF value is equal to 0.802, which is lower than the TF value obtained against photons at 0.678 MeV with shields 0.5 cm thick. Therefore, to lower the TF values as much as possible, the BaO content and thickness should both be increased.

Figure 5 shows the ratio of HVL values between the S1 glass and S4 glass at several energies. At all energies, the ratio remains above one, showing that S1's HVL always remains greater than S4's HVL. The ratio starts out at 1.095, dropping down to 1.086, before oscillating at higher energies. These fluctuations show that at certain energies there is a smaller advantage for the S4 sample compared to the S1 sample. Nevertheless, at all energies, the greater the BaO content in the system, the better the shielding capabilities of the glass.

The TVL of the samples is shown in Fig. 6 against energy. At low energies, the TVL values are very close together, and spread further apart as the radiation energy increases.

For example, at 0.122 MeV, the TVL values are equal to 0.346, 0.329, 0.314, and 0.300 cm for S1, S2, S3, and S4, respectively. At 0.678 MeV they are equal to 6.144, 5.945, 5.758, and 5.582 cm, respectively, while at 1.458 MeV, they are 10.446, 10.121, 9.815, and 9.527 cm, respectively. This trend first demonstrates that the samples with more BaO content outperform the samples with more B_2O_3. Additionally, the greater the photon energy, the more that the high BaO concentration glasses have an advantage, demonstrating the desirability of the S4 glass over the other shields.

Figure 7 shows the relationship between the MFP of the glasses and their density at several energies. The values demonstrate that the greater the energy of the incoming photons, the higher the MFP values. For example, at a density of 4.275 g/cm^3, the MFP values are equal to 0.150, 1.750, 3.493, and 4.537 cm at 0.122, 0.444, 0.964, and 1.458 MeV, respectively, while at a density of 4.764 g/cm^3 the MFP values at the same respective energy are equal to 0.137, 1.608, 3.190, and 4.137 cm. Like for TF, the higher energy photons have a greater penetration power, leading to a lower MFP at any set density. To lower the MFP value though, the density of the samples can be increased. For example, at 0.344 MeV, the MFP values are equal to 1.249, 1.203, 1.160, and 1.120 cm at densities of 4.275, 4.438, 4.601, and 4.764 g/cm^3, respectively, while at 1.005 MeV they are equal to 3.596, 3.483, 3.378, and 3.278 cm, respectively. Because of this trend, the S4 sample, having the highest BaO concentration and greatest density, has the lowest MFP value.

The Z_{eff} of the glasses was next evaluated against energy in Fig. 8. The figure shows a rapid decrease in values at low energies, which is caused by the photoelectric effect, followed by a slower decrease in values caused by the Compton scattering effect. For example, for the S2 sample, its Z_{eff} values are equal to 55.52, 31.76, 26.85, and 23.76 at 0.122, 0.245, 0.296, and 0.344 MeV, followed by 20.04, 16.66, 16.02, and 15.63 at 0.444, 0.678, 0.779, and 0.867 MeV, respectively. The relationship between the Z_{eff} values and the energies are directly related to the relationship that each of the photon interaction phenomena have with energy. Furthermore, at both energy ranges, the S4 glass has the greatest Z_{eff} value. For instance, at 0.245 MeV, the Z_{eff} values are equal to 30.10, 31.76, 33.47, and 35.21 for S1-S4, while at 1.005 MeV they are respectively equal to 14.16, 15.20, 16.33, and 17.56. Therefore, the S4 glass, which has the greatest BaO content and least B_2O_3 concentration, has the most desirable Z_{eff} at all energies.

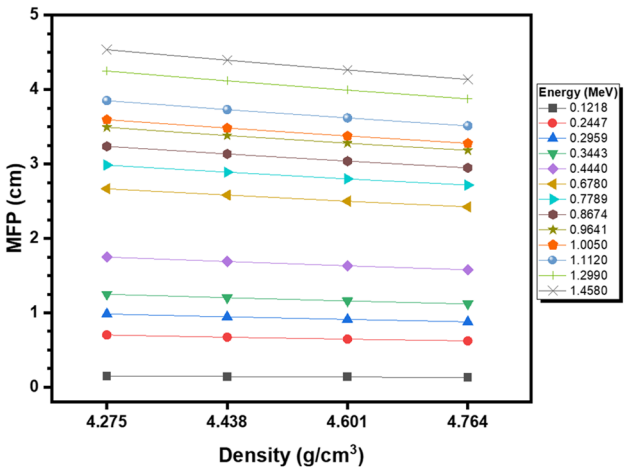

Fig. 7 the relationship between the MFP of the glasses and their density at several energies

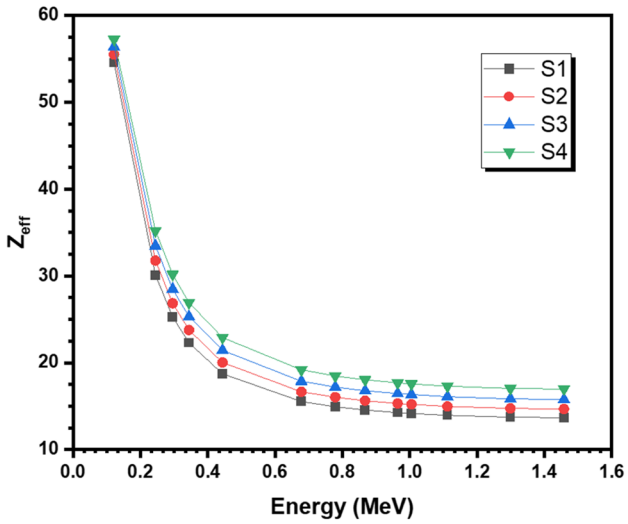

Fig. 8 The effective atomic number of the glasses against the energy of the radiation

4 Conclusion

We successfully prepared a glass sample series with the chemical compositions 5MgO-20PbO-10SiO_2-(65-x)B_2O_3-xBaO, (x = 10, 15, 20 and 25 mol%). The glasses' capacity for radiation shielding was investigated through the Phy-X software. The addition of BaO leads to a notable LAC improvement, corroborating the enhanced radiation shielding features of BaO-enriched glasses. Moreover, our investigation into the impact of energy of the photon and the thickness of the samples on TF revealed a reduction in TF with increasing thickness, confirming the positive role of the thickness of the glasses on radiation shielding abilities. The glasses' HVL and TVL were examined and both parameters were found to decrease due to the addition of BaO. At 0.122 MeV, the TVL values are 0.346, 0.329, 0.314, and 0.300 cm respectively for S1 to S4. At 0.678 MeV they are 6.144, 5.945, 5.758, and 5.582 cm, respectively. According to the MFP results, the greater the incoming photon energy, the

higher the MFP values. Also, to lower the MFP value, the samples' density can be enhanced.

Authors' Contribution Writing the first draft of the manuscript and reviewing-editing were performed by M. I. Sayyed. All authors reviewed the manuscript.

Funding None.

Data Availability No datasets were generated or analysed during the current study.

Code Availability Not applicable.

Declarations

Ethics Approval Not applicable.

Consent to Participate Not applicable.

Consent for Publication Not applicable.

Competing Interests The authors declare no competing interests.

References

1. Alzahrani FMA, Elqahtani ZM, Alzahrani JS, Eke C, Alrowaili ZA, Al-Buriahi MS (2024) Gamma attenuation characteristics of silicon-rich glasses in Na2O–SiO2–Al2O3–CaO–ZnO system for radiation applications. J Radiat Res Appl Sci 17(1):100760
2. Olarinoye IO, Rammah YS, Alraddadi S, Sriwunkum C, Abd El-Rehim AF, Zahran HY, Al-Buriahi MS (2020) The effects of La2O3 addition on mechanical and nuclear shielding properties for zinc borate glasses using Monte Carlo simulation. Ceram Int 46(18):29191–29198
3. Al-Buriahi MS, Alrowaili ZA, Alsufyani SJ, Olarinoye IO, Alharbi AN, Sriwunkum C, Kebaili I (2022) The role of PbF2 on the gamma-ray photon, charged particles, and neutron shielding prowess of novel lead fluoro bismuth borate glasses. J Mater Sci Mater Electron 33(3):1123–1139
4. Naseer KA, Marimuthu K, Mahmoud KA, Sayyed MI (2021) Impact of Bi2O3 modifier concentration on barium–zincborate glasses: physical, structural, elastic, and radiation-shielding properties. Eur Phys J Plus 136:116
5. Alalawi A, Al-Buriahi MS, Sayyed MI, Akyildirim H, Arslan H, Zaid MHM, Tonguc BT (2020) Influence of lead and zinc oxides on the radiation shielding properties of tellurite glass systems. Ceram Int 46(11):17300–17306
6. Al-Buriahi MS, Taha TA, Alothman MA, Donya H, Olarinoye IO (2021) Influence of WO3 incorporation on synthesis, optical, elastic and radiation shielding properties of borosilicate glass system. Eur Phys J Plus 136(7):779
7. Pacheco MH, Gibin MS, Silva MA, Montagnini G, Viscovini RC, Steimacher A, Pedrochi F, Zanuto VS, Muniz RF (2023) BaO–reinforced SiO2–Na2O–Ca(O/F2)–Al2O3 glasses for radiation safety: On the physical, optical, structural and radiation shielding properties. J Alloy Compd 960:171019
8. Katubi KM, Alsulami RA, Albarqi MM, Alrowaili ZA, Kebaili I, Singh VP, Al-Buriahi MS (2024) Radiation Shielding efficiency of lead-tungsten-boron glasses with Sb, Al, and Bi against gamma, neutron and charge particles. Appl Radiat Isot 204:111139
9. Al-Buriahi MS, Alrowaili ZA, Eke C, Alzahrani JS, Olarinoye IO, Sriwunkum C (2022) Optical and radiation shielding studies on tellurite glass system containing ZnO and Na2O. Optik 257:168821
10 Issa SAM, Rashad M, Hanafy TA, Saddeek YB (2020) Experimental investigations on elastic and radiation shielding parameters of WO3-B2O3-TeO2 glasses. J Non-Cryst Solids 544:120207
11. Al-Buriahi MS, Alzahrani JS, Olarinoye IO, Akyildirim H, Alomairy S, Kebaili I, Tekin HO, Mutuwong C (2021) Role of heavy metal oxides on the radiation attenuation properties of newly developed TBBE-X glasses by computational methods. Physica Scripta 96(7):075302
12. Alrowaili ZA, Al-Baradi AM, Sayed MA, Ali AM, Abdel Wahab EA, Al-Buriahi MS, Shaaban Kh. S (2022) The impact of Fe2O3 on the dispersion parameters and gamma/fast neutron shielding characteristics of lithium borosilicate glasses. Optik 249:168259
13. Tamam N, Alrowaili ZA, Olarinoye IO, Hammoud A, Albarkaty KS, Kebaili I, Al-Buriahi MS (2024) Fabrication and characterisation of TeO2-based composite doped with Yb3+ and Bi3+ for enhanced radiation shielding safety. Radiat Phys Chem 215:111315
14. Mhareb MHA (2023) Optical, Structural, Radiation shielding, and Mechanical properties for borosilicate glass and glass ceramics doped with Gd2O3. Ceram Int 49(22):36950–36961
15. Hanfi MY, Sayyed MI, Lacomme E, Akkurt I, Mahmoud KA (2021) The influence of MgO on the radiation protection and mechanical properties of tellurite glasses. Nucl Eng Technol 53:2000–2010
16. Aşkın A, Sayyed MI, Dal Amandeep Sharma M, El-Mallawany R, Kaçal MR (2019) Investigation ofthe gamma ray shielding parameters of (100–x) [0.5Li2O–0.1B2O3–0.4P2O5]-xTeO2 glasses using Geant4 and FLUKA codes. J Non-Cryst Solids 521:119489
17. Abouhaswa AS, Kavaz E (2020) Bi2O3 effect on physical, optical, structural and radiation safety characteristics of B2O3-Na2O-ZnO-CaO glass system. J Non-Cryst Solids 535:119993
18 Abouhaswa AS, Kavaz E (2020) A novel B_2O_3-Na_2O-BaO-HgO glass system: Synthesis, physical, optical and nuclear shielding features. Ceram Int 46:16166–16177
19. Sayyed MI (2024) Effect of WO3 on the attenuation parameters of TeO2–La2O3-WO3 glasses for radiation shielding application. Radiat Phys Chem 215:111319
20. Sayyed MI (2022) The role of Bi2O3 on radiation shielding characteristics of ternary bismuth tellurite glasses. Optik 270:169973
21. Saleh A, Shalaby RM, Abdelhakim NA (2022) Comprehensive study on structure, mechanical and nuclear shielding properties of lead free Sn–Zn–Bi alloys as a powerful radiation and neutron shielding material. Radiat Phys Chem 195:110065. https://doi.org/10.1016/j.radphyschem.2022.110065
22. Saleh A, El-Feky MG, Hafiz MS, Kawady NA (2022) Experimental and theoretical investigation on physical, structure and protection features of TeO2-B2O3 glass doped with PbO in terms of gamma, neutron, proton and alpha particles. Radiat Phys Chem 202:110586. https://doi.org/10.1016/j.radphyschem.2022.110586
23. Almuqrin AH, Sayyed MI (2021) Radiation shielding characterizations and investigation of TeO2–WO3–Bi2O3 and TeO2–WO3–PbO glasses. Appl Phys A 127:190
24. Şakar E, Özpolat ÖF, Alım B, Sayyed MI, Kurudirek M (2020) Phy-X / PSD: Development of a user friendly online software for calculation of parameters relevant to radiation shielding and dosimetry. Radiat Phys Chem 166:108496
25. Alrowaili ZA, Taha TA, Ibrahim M, Saron KMA, Sriwunkum C, Al-Baradi AM, Al-Buriahi MS (2021) Synthesis and characterization of B2O3-Ag3PO4-ZnO-Na2O glasses for optical and radiation shielding applications. Optik 248:168199
26. Singh J, Kumar V, Vermani YK, Al-Buriahi MS, Alzahrani JS, Singh T (2021) Fabrication and characterization of barium based

bioactive glasses in terms of physical, structural, mechanical and radiation shielding properties. Ceram Int 47(15):21730–21743
27. Edukondalu A, Stalin S, Srinivasa Reddy M, Eke C, Alrowaili ZA, Al-Buriahi MS (2022) Synthesis, thermal, optical, mechanical and radiation-attenuation characteristics of borate glass system modified by Bi2O3/MgO. Appl Phys A 128(4):331
28. Zughbi A, Kharita MH, Shehada AM (2017) Determining optical and radiation characteristics of cathode ray tubes' glass to be reused as radiation shielding glass. Radiat Phys Chem 136:71–74
29. Alzahrani JS, Alrowaili ZA, Olarinoye IO, Alothman MA, Al-Baradi AM, Kebaili I, Al-Buriahi MS (2021) Nuclear shielding properties and buildup factors of Cr-based ferroalloys. Prog Nucl Energy 141:103956
30. Aliyah F, Kambali I, Setiawan AF, Radzi YMd, Rahman AA (2023) Utilization of steel slag from industrial waste for ionizing radiation shielding concrete: A systematic review. Construct Build Mater 382:131360
31. Al-Buriahi MS, Alrowaili ZA, Alomairy S, Olarinoye IO, Mutuwong C (2022) Optical properties and radiation shielding competence of Bi/Te-BGe glass system containing B2O3 and GeO2. Optik 257:168883
32. Sayyed MI (2023) Exploring the Impact of PbO in Improving the Gamma Radiation Shielding Characteristics of Silicate Glasses. Silicon. https://doi.org/10.1007/s12633-023-02776-x
33. Al-Buriahi MS (2023) Radiation shielding performance of a borate-based glass system doped with bismuth oxide. Radiat Phys Chem 207:110875
34. Al Huwayz M, Albarkaty KS, Alrowaili ZA, Olarinoye IO, Elqahtani ZM, Al-Buriahi MS (2023) Gamma, neutron, and charged particle shielding performance of ABKT glass system. J Radiat Res Appl Sci 16(4):100742
35 Shaaban Kh S, Tamam N, Alghasham HA, Alrowaili ZA, Al-Buriahi MS, Ellakwa TE (2023) Thermal, optical, and radiation shielding capacity of B2O3-MoO3-Li2O-Nb2O5 glasses. Mater Today Commun 37:107325
36. Alzahrani JS, Yilmaz E, Çalişkan F, Alrowaili ZA, Olarinoye IO, Alqahtani MS, Arslan H, Al-Buriahi MS (2023) Synthesis and optimization of B2O3-based glass: Influence of MgO on hardness, structure properties, and radiation shielding performance. Mater Today Commun 37:106933
37. Alzahrani JS, Alrowaili ZA, Alqahtani MS, Eke C, Olarinoye IO, Adam M, Al-Buriahi MS (2023) Influence of alkaline earth metals on the optical properties and radiation-shielding effectiveness of Sm3+-doped zinc borophosphate glasses. J Electron Mater 52(11):7794–7806
38. Mahmoud KA, Abu El-Soad AM, Kovaleva EG, Tashlykov OL (2022) Modeling a three-layer container based on halloysite nanoclay for radioactive waste disposal. Prog Nucl Energy 152:104379
39. Ekinci N, Mahmoud KA, Aygün B, Hessien MM, Rammah YS (2022) Impacts of the colemanite on the enhancement of the radiation shielding capacity of polypropylene. J Mater Sci Mater Electron 33(25):20046. https://doi.org/10.1007/s10854-022-08822-5
40. Mahmoud KG, Alqahtani MS, Tashlykov OL, Semenishchev VS, Hanfi MY (2023) The influence of heavy metallic wastes on the physical properties and gamma-ray shielding performance of ordinary concrete: experimental evaluations. Radiat Phys Chem. 206:110793
41. Hanfi MY, Sakr AK, Ismail AM, Atia BM, Alqahtani MS, Mahmoud KA (2023) Physical characterization and radiation shielding features of B2O3-As2O3 glass ceramic. Nucl Eng Technol 55(1):278–284
42. Sayyed MI (2024) Radiation shielding characterization of a Yb:CaBTeX glass system as a function of TeO2 concentration. Opt Quant Electron 56:333